

Electron-nuclear double resonance of $^{53}\text{Cr}^{3+}$ in guanidinium aluminum sulfate hexahydrate

A. Manoogian and A. Leclerc

Department of Physics, University of Ottawa, Ottawa K1N 6N5, Canada

(Received 25 September 1973)

Electron-nuclear-double-resonance (ENDOR) studies are reported for the isotope $^{53}\text{Cr}^{3+}$ enriched to 96% in guanidinium aluminum sulfate hexahydrate (GAlSH). The measurements were done at 4.2 °K and X-band microwave frequencies (~ 9.4 GHz). The study allowed accurate values of the spin-Hamiltonian hyperfine parameters to be determined and ENDOR patterns to be classified. The sign of the zero-field splitting parameter D was found to be negative, where previously only a positive relative value had been quoted. A linear relationship was found when plotting values of Q' vs $A-B$, utilizing data obtained in GAlSH and previous results of RbGa and CsGa alums. The best value of the quadrupole moment of ^{53}Cr was determined to be $Q = -0.028 \pm 0.005$ b.

I. INTRODUCTION

Electron-nuclear-double-resonance (ENDOR) experiments were carried out on $^{53}\text{Cr}^{3+}$ ions doped in single crystals of guanidinium aluminum sulfate hexahydrate (GAlSH), $\text{C}(\text{NH}_2)_3\text{Al}(\text{SO}_4)_2 \cdot 6\text{H}_2\text{O}$. The chromium dopant was 96% enriched $^{53}\text{Cr}^{3+}$ isotope with a concentration of less than 0.01 wt% in the crystals. The crystals were colorless and grew from aqueous solution, exhibiting the usual hexagonal plates with flat faces parallel to $\{0001\}$. The measurements were done at 4.2 °K and X-band microwave frequency (~ 9.4 GHz). The experimental equipment used has been described previously.^{1,2}

Crystallographic studies³⁻⁷ of GAlSH and its isomorphs have illuminated the structure and properties of this material. It was found to be ferroelectric with space group $C_{3v}^2(P31m)$, and containing three molecules per unit cell. The direction of spontaneous polarization is along the c axis of the crystal. The polarization appears to exist for all temperatures where the crystal is stable. The measurements of Holden *et al.*,⁵ in the range 90–50 °C, show that the spontaneous polarization increases in magnitude with decreasing temperature. Each Al ion in GAlSH is surrounded by an octahedron of water molecules which is trigonally distorted by a slight compression along the crystal c axis. Furthermore, each Al ion is displaced somewhat along the c axis from the center of the octahedron. Two of the three Al complexes are crystallographically equivalent. The ferroelectric mechanism in GAlSH was attributed by Schein *et al.*⁸ to c -axis displacements of the atomic parameters which are not related by a center of symmetry and are not compensated for by displacements in the opposite direction. These conditions are found to hold for the three Al complexes.

The electron-spin resonance (ESR) of Cr^{3+} in GAlSH and its isomorphs was studied by a number

of authors.⁹⁻¹³ Two nonequivalent magnetic complexes exhibiting axial symmetry about the c axis were found. The ESR lines of one complex have twice the intensity of the other, indicating that the former consists of two equivalent complexes. This result is consistent with the crystallographic data. The work of Daniels *et al.*,¹⁰ in the range 295–35 °K, shows that the D -spin-Hamiltonian parameter of each complex increases almost linearly as the temperature is lowered. The work of Milsch *et al.*¹² involves the study of the satellite lines which also occur in the ESR spectrum.

The purpose of the present work is to obtain precise values of the spin-Hamiltonian hyperfine parameters of $^{53}\text{Cr}^{3+}$ in GAlSH in order to determine the behavior of the crystal and the applicability of the theory. The GAlSH crystal is particularly interesting because (i) the chromium sites have axial symmetry and hence can be more easily studied; (ii) the D -spin-Hamiltonian parameters increase with decreasing temperature, which is the reverse of what usually happens in most crystals; and (iii) the crystal is ferroelectric. One would like to know if the increase of the D parameter is related to the ferroelectric behavior of the crystal, and in fact if the ferroelectric property manifests itself in any way in the ENDOR results.

ENDOR of $^{53}\text{Cr}^{3+}$ in hydrated salts was done previously by Danilov and Manoogian² in the gallium alums $\text{RbGa}(\text{SO}_4)_2 \cdot 12\text{H}_2\text{O}$ and $\text{CsGa}(\text{SO}_4)_2 \cdot 12\text{H}_2\text{O}$. The Ga ions in the alums are coordinated by nearly-regular octahedrons of water molecules. The Cr^{3+} impurities which replace Ga were found to be subjected to a trigonal distortion along the crystal $\langle 111 \rangle$ direction. Values of the D -spin-Hamiltonian parameters in the gallium alums and in GAlSH are of the same order of magnitude at 295 °K. In the gallium alums, it was postulated on the basis of assumptions regarding the crystalline electric field at the chromium sites that the quadrupole moment of ^{53}Cr is $Q = -0.035 \pm 0.005$ b. The additional GAlSH ENDOR results indicate that the previous

assumptions are probably true and that the quadrupole moment is reduced slightly from the above value.

II. RESULTS

The spin Hamiltonian used to describe the resonance results is of the form

$$\begin{aligned} \mathcal{H}_S = & g_{\parallel}\mu_B S_z H_z + g_{\perp}\mu_B (S_x H_x + S_y H_y) \\ & + D[S_z^2 - \frac{1}{3}S(S+1)] + AS_z I_z + B(S_x I_x + S_y I_y) \\ & + Q'[I_z^2 - \frac{1}{3}I(I+1)] - g'_{\parallel}\mu_N I_z H_z \\ & - g'_{\perp}\mu_N (I_x H_x + I_y H_y). \end{aligned} \quad (1)$$

The first three terms of Eq. (1) are the usual fine-structure terms used in ESR, while the last five terms are the hyperfine terms which are evaluated in the ENDOR work. The ground state of $^{53}\text{Cr}^{3+}$ is described by the quantum numbers $S = \frac{3}{2}$ and $I = \frac{3}{2}$, and so the Hamiltonian can be represented by a 16×16 matrix. The rotation of the above Hamiltonian by 90° to a perpendicular direction has been described previously.^{14,15}

A. ESR results

Prior to performing ENDOR it is necessary to study the ESR of Cr^{3+} so as to determine the pertinent g values and D parameters of the chromium complexes in the particular GALSH crystals grown. This was done on crystals doped with Cr^{3+} in its natural isotopic form and with the $^{53}\text{Cr}^{3+}$ isotope enriched to 96%. The study was done both at 295 and 4.2°K.

The usual two chromium magnetic complexes exhibiting axial symmetry about the crystal c axis were found in the ESR work. No differences in the g and D values were found due to the isotopic form of the chromium. Typical ESR spectra obtained at 295°K for the natural chromium isotope when the magnetic field was set along the z axis and along a perpendicular direction are shown in Figs. 1(a) and 1(b), respectively. ESR lines belonging to the two complexes are labeled $G(1)$ and $G(2)$. The spectra obtained for $^{53}\text{Cr}^{3+}$ are the same as shown in Fig. 1 except that each fine-structure line now consists of a group of four hyperfine lines as shown in Fig. 2. Magnetic-field measurements were made at the center of the hyperfine group in the ESR work, and at the positions marked H_1 , H_2 , and H_3 in the ENDOR work when operating at 4.2°K.

The ESR lines obtained for $^{53}\text{Cr}^{3+}$ in GALSH at 4.2°K are shown in Fig. 3. It is seen here that the groups of hyperfine lines appear at the tops of large bulges. The reason for the bulges is uncertain, but it was noted that they were always larger for the high-field lines than for the low-field lines along both the z and perpendicular directions. Their presence was found to be typical for GALSH, and we did not observe this behavior previously

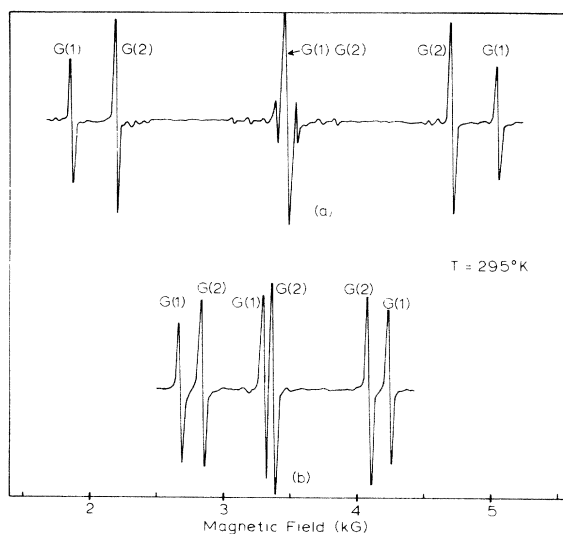


FIG. 1. Cr^{3+} ESR fine-structure spectra obtained in GALSH at 295°K when the magnetic field was set (a) along the z axis (crystal c axis) and (b) along a perpendicular direction. The lines for the two inequivalent magnetic complexes are denoted by $G(1)$ and $G(2)$.

when working with alums. The presence of bulges did not cause any difficulty when obtaining ENDOR results, but one must be careful in obtaining the sign of the D parameter when comparing the relative intensities of the low- and high-field lines from the z -axis spectrum at 4.2°K. By studying only the intensities of the hyperfine lines, which ride on top of the bulges, it is observed that the low-field lines have a greater intensity than the high-field lines in the proportion 1.4:1. This fixes the sign of D to be negative for both complexes.

The calculated values of g and D are listed in Table I. The fine-structure energy-level diagram for the $G(1)$ complex at 295°K is shown in Fig. 4. It is seen in Table I that the g values are essentially isotropic and the same for both complexes, while the D values increase with decreasing temperature. The percentage changes in D , i.e., $(100\Delta D)/D_{4.2^\circ\text{K}}$, are found to be 36.6% for complex $G(1)$ and 35.1% for $G(2)$, which are nearly identical.

B. ENDOR results

ENDOR measurements were made at 4.2°K in the 75-MHz range on the low- and high-field groups of hyperfine lines for each magnetic complex, in both the z and perpendicular directions. Typical chart recordings of the z -axis ENDOR spectra of complex $G(1)$ for magnetic-field settings on the low-field group of hyperfine lines ($M_s = -\frac{3}{2} \rightarrow -\frac{1}{2}$) and on the high-field group ($M_s = \frac{3}{2} \rightarrow \frac{1}{2}$) are

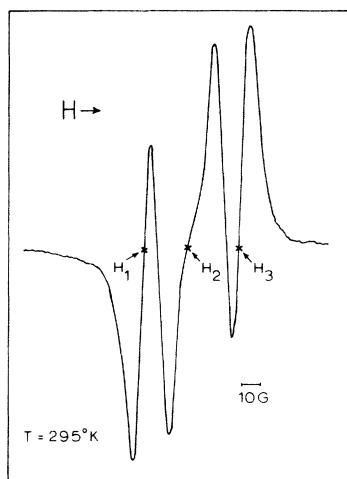


FIG. 2. ESR spectrum of a typical group of four hyperfine lines of $^{53}\text{Cr}^{3+}$ when this isotope is doped in the GAlSH crystal. This particular spectrum is taken from the low-field line of complex G(1) on the z axis at 295 °K. ESR magnetic-field measurements were obtained at the center of the packet, marked H_2 , while ENDOR measurements were obtained at the three points marked H_1 , H_2 , and H_3 when working at 4.2 °K.

shown in Figs. 5 and 6, respectively. These results are classified in Fig. 7. Essentially, the same results are obtained for complex G(2), there being no qualitative difference between the two complexes. The method of parameter fitting was as follows: The values of g_{\parallel} , g_{\perp} , and D were obtained from the ESR measurements. The spin Hamiltonian of Eq. (1) was then diagonalized using second-order perturbation theory to give a set of equations which were solved to give rough values

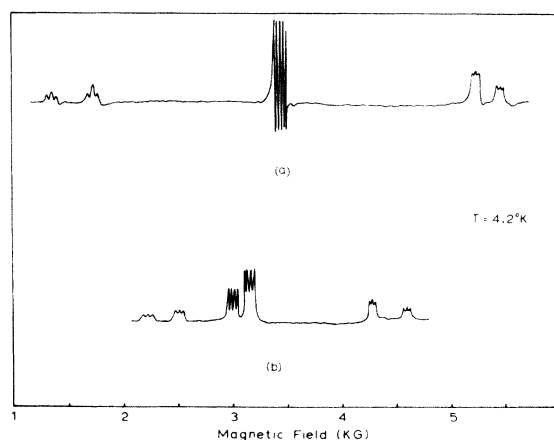


FIG. 3. $^{53}\text{Cr}^{3+}$ ESR spectra obtained in GAlSH at 4.2 °K when the magnetic field was set (a) along the z axis (crystal c axis) and (b) along a perpendicular direction.

of A , B , Q' , and g'_n when utilizing the z -axis ENDOR data. These values were then used as a starting point for exact diagonalization of the spin-Hamiltonian matrices for the z and perpendicular directions using an IBM 360 diagonalization subroutine. The final values of the parameters are listed in Table I. The ENDOR results were fitted with an average error of 7 kHz, which was consistent with the accuracy of the experimental measurements.

III. DISCUSSION AND CONCLUSIONS

The D parameter was found to be negative. In other chromium ESR work^{10,11} in GAlSH where measurements were made at low temperature (but

TABLE I. Spin-Hamiltonian parameters of $^{53}\text{Cr}^{3+}$ in GAlSH.

Spin-Hamiltonian parameter	Complex G(1)		Complex G(2)	
	295 °K	4.2 °K	295 °K	4.2 °K
g_{\parallel} (± 0.0005)	1.9788	1.9782	1.9784	1.9783
g_{\perp} (± 0.0008)	1.9781	1.9784	1.9781	1.9775
D (10^{-4} cm $^{-1}$) (± 5.0)	-733.0	-1,155.3	-577.2	-888.7
A (10^{-4} cm $^{-1}$) (± 0.0005)		17.0774		17.0982
B (10^{-4} cm $^{-1}$) (± 0.0005)		17.4273		17.4236
Q' , (10^{-4} cm $^{-1}$) (± 0.0010)		0.1682		0.1866
g'_n (± 0.0005)		-0.3165		-0.3165

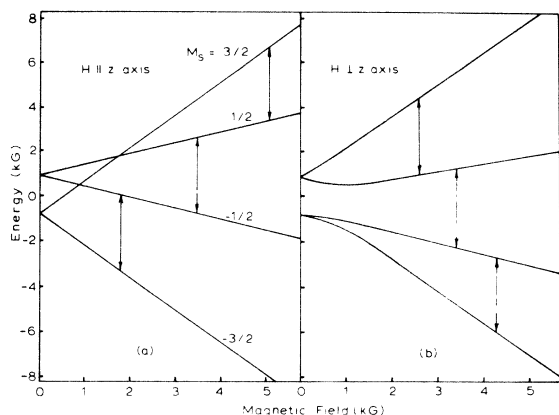


FIG. 4. Cr^{3+} fine-structure energy-level diagram of the complex $G(1)$ when the magnetic field was set (a) along the z direction and (b) along a perpendicular direction for measurements at 295°K .

not as low as 4.2°K) the D value was assumed to be positive. Presumably those authors refer to only the relative sign of D . The negative- D value fits into the theoretical framework of McGarvey¹⁶ which correlates the relative magnitudes of the A and B hyperfine parameters and the axial extension or compression of the octahedron of waters surrounding the chromium ion.

McGarvey¹⁶ has given the following expressions which describe the A and B parameters:

$$A = P \left[\frac{4}{21} (1 - 2a^2 + b^2) - K \right], \quad (2)$$

$$B = P \left[-\frac{2}{21} (1 - 2a^2 + b^2) - K \right]. \quad (3)$$

Here $P = -40 \times 10^{-4} \text{ cm}^{-1}$ for $^{53}\text{Cr}^{3+}$; the first term in the square brackets arises from the electron-nuclear dipole-dipole interaction, while the K represents the contribution due to the Fermi contact term. For a site with octahedral symmetry of the coordinated ligands we have $a^2 = \frac{2}{3}$, $b^2 = \frac{1}{3}$, and $1 - 2a^2 + b^2 = 0$, giving $A = B$ from Eqs. (2) and (3). In this case, the hyperfine interaction is iso-

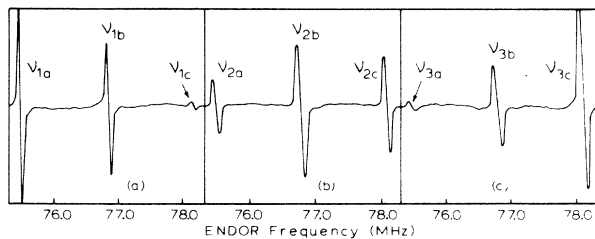


FIG. 5. ENDOR spectra obtained along the z axis for the low-field group of hyperfine lines of complex $G(1)$; (a), (b), and (c) are the spectra obtained when the magnetic field was set on positions H_1 , H_2 , and H_3 , respectively, as indicated in Fig. 2. The description of frequencies ν_{1a} , ν_{1b} , etc., is explained in Fig. 7.

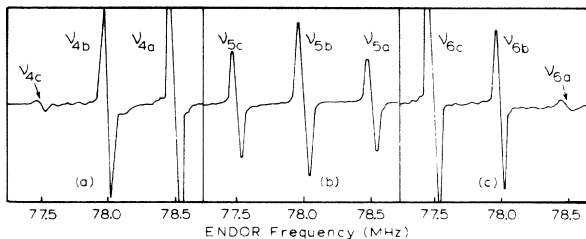


FIG. 6. ENDOR spectra obtained along the z axis for the high-field group of hyperfine lines of complex $G(1)$; (a), (b) and (c) are the spectra obtained when the magnetic field was set on the low-, middle-, and high-field positions, respectively, of the hyperfine group.

tropic and is given by PK . If $a^2 < \frac{2}{3}$ and $b^2 > \frac{1}{3}$ then $1 - 2a^2 + b^2$ is positive and $A < B$. McGarvey¹⁷ shows that the D parameter is negative for this case and the coordinated octahedron is trigonally compressed. If $a^2 > \frac{2}{3}$ and $b^2 < \frac{1}{3}$ then $1 - 2a^2 + b^2$ is negative, giving $A > B$. This case corresponds to a positive D and a trigonal extension of the octahedron.

In the analysis which follows we include the results found previously for gallium alums,² since this gives us more data to work with when attempting to fit the ENDOR results to the simple theory. Also, it is possible to check if the various assumptions made in the case of gallium alums are true. In this respect, the pertinent spin-Hamiltonian parameters and other data calculated for the two types of crystals are listed in Table II.

Subtracting Eqs. (2) and (3) we obtain the expression $A - B = \frac{2}{21} P (1 - 2a^2 + b^2)$, which allows the value of $1 - 2a^2 + b^2$ to be calculated. As seen in Table II the experimental values of $A - B$ are negative for GAlSH, and so $1 - 2a^2 + b^2$ is positive since P is negative. This corresponds to $a^2 < \frac{2}{3}$ and is related to a negative- D value consistent with McGarvey's theory. The results are also consistent with the fact that the octahedron of waters surrounding a Cr or Al site in GAlSH exhibit a trigonal compression.⁷ Adding Eqs. (2) and (3) we obtain the relation $A + B = 2P \left[\frac{1 - 2a^2 + b^2}{21} - K \right]$, which allows the K values to be calculated. These values are listed in Table II, and they are seen to be essentially identical to the values obtained in the alums.

The following simple relation has been given¹⁸ for the D parameter and the electric-field gradient V_{zz} due to charges and dipoles external to the Cr ion:

$$D = \frac{3}{7} (\lambda / \Delta E)^2 \langle r^{-2} \rangle V_{zz} \quad (4)$$

The quantity λ is the spin-orbit coupling constant of Cr in the crystal, E is the energy separation between the ground state 4A_2 and the excited state

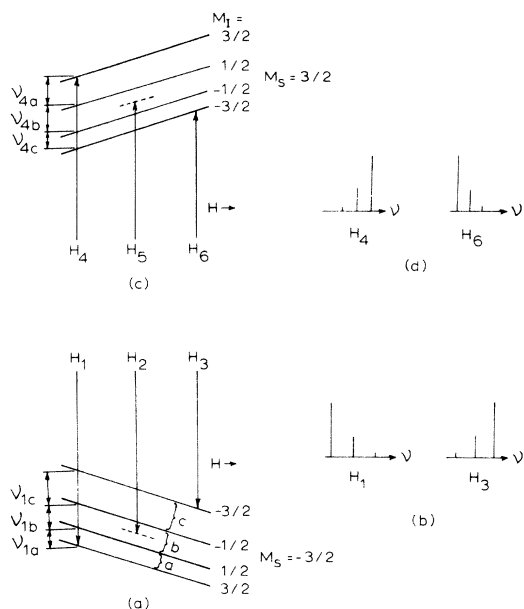


FIG. 7. Classification of the key z -direction ENDOR lines of the $G(1)$ complex; (a) represents the $M_s = -\frac{3}{2} \rightarrow -\frac{1}{2}$ hyperfine lines, (b) gives the relative positions and intensities of the ENDOR lines obtained when the magnetic field was set at the H_1 and H_3 positions, (c) represents the $M_s = \frac{3}{2} \rightarrow \frac{1}{2}$ hyperfine lines, and (d) gives the relative positions and intensities of the ENDOR lines obtained when the magnetic field was set on the H_4 and H_6 positions.

4T_2 , and $\langle r^2 \rangle$ is the average value of r^2 for the Cr^{3+} $3d$ wave function. Values of V_{zz} for GAlSH are calculated using $\lambda = 87 \text{ cm}^{-1}$, $\Delta E = 17320 \text{ cm}^{-1}$, $\langle r^2 \rangle = 1.447 \text{ a.u.}$, and the $D_{4.2^\circ\text{K}}$ values. These results are listed in Table II along with the values previously calculated for the gallium alums.²

The nuclear quadrupole interaction constant Q' in the spin Hamiltonian can be written in terms of the quadrupole moment eQ of ${}^{53}\text{Cr}$ as

$$Q' = [3V_{zz}eQ/4I(2I-1)](1-\gamma_\infty), \quad (5)$$

TABLE II. Tabulation of some GAlSH and alum^a ${}^{53}\text{Cr}^{3+}$ spin-Hamiltonian parameters and other relationships obtained at 4.2°K .

Parameter or relation	GAlSH (G1)	GAlSH (G2)	RbGa(SO ₄) ₂ · 12H ₂ O	CsGa(SO ₄) ₂ · 12H ₂ O
$A(10^{-4} \text{ cm}^{-1})$	17.0774	17.0982	17.3722	17.2119
$B(10^{-4} \text{ cm}^{-1})$	17.4273	17.4236	17.2914	17.4754
$A-B(10^{-4} \text{ cm}^{-1})$	-0.3499	-0.3254	0.0808	-0.2635
$A+B(10^{-4} \text{ cm}^{-1})$	34.5047	34.5218	34.6636	34.6873
$Q'(10^{-4} \text{ cm}^{-1})$	0.1682	0.1866	-0.0164	0.1546
$D(10^{-4} \text{ cm}^{-1})$	-1,155.3	-888.7	534.2	-670.1
$1-2a^2+b^2$	0.0307	0.0285	-0.0071	0.0231
K	0.433	0.433	0.433	0.435
$V_{zz}(10^{-4} \text{ cm}^{-1}/b)$	-2.637	-2.029	1.287	-1.597
$Q(b)$	-0.021	-0.031	-0.0042	-0.032

^aAfter Danilov and Manoogian, Ref. 2.

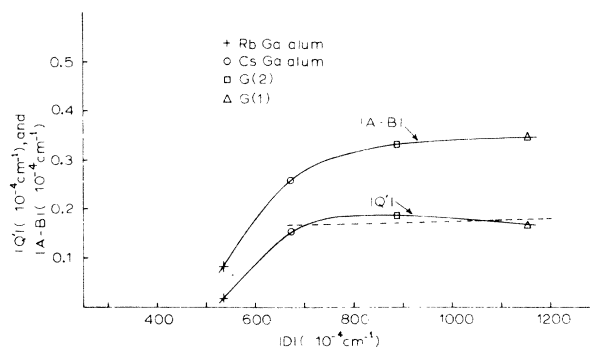


FIG. 8. Plot of $|Q'|$ and $|A-B|$ vs $|D|$ for the two GAlSH complexes $G(1)$, $G(2)$, and including CsGa alum and RbGa alum, utilizing results obtained at 4.2°K .

where V_{zz} is the electric field gradient external to the chromium ion, and $1-\gamma_\infty$ is the Sternheimer antishielding factor for Cr^{3+} with a value¹⁹ 12.0 ± 1.0 . Using the values of V_{zz} found from Eq. (4) it is possible to calculate corresponding values of Q , and these are listed in Table II. It is interesting to note that the Q values obtained for the two complexes in GAlSH are similar to the value obtained in CsGa alum. In the analysis of the gallium alum ENDOR work² it was stated on the basis of assumptions regarding the behavior of the alums that the value found for CsGa alum was probably the correct one. The value found for RbGa alum was considered to be too small because Eq. (4) did not predict the correct value of V_{zz} .

It would appear that Eq. (4) applies only in a limited range of D vs V_{zz} . This effect is shown in Fig. 8 where the absolute values of $|D|$ are plotted against $|A-B|$ and $|Q'|$. The dotted line in this figure indicates where $|Q'| \propto |D|$ holds, or alternatively, $|V_{zz}| \propto |D|$. Figure 8 shows an interesting feature which includes the RbGa alum data, and that is the empirical fact that the $|A-B|$ curve follows the $|Q'|$ curve very closely. To show this

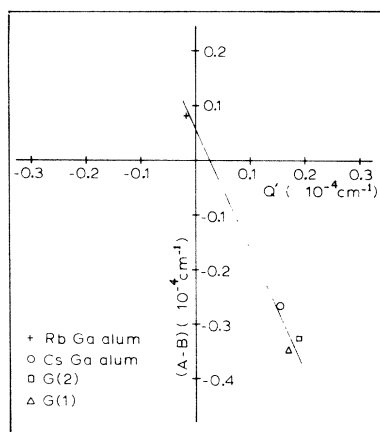


FIG. 9. Plot of $A-B$ vs Q' for the two GAlSH complexes $G(1)$, $G(2)$, and including CsGa alum and RbGa alum, utilizing results obtained at 4.2°K .

effect more clearly, values of $A - B$ vs Q' are plotted in Fig. 9. Here it is seen that all the points fall close to a straight line, and this result is consistent even when the relative signs of $A - B$ and Q' are accounted for. Within restrictions of the limited number of points which make up Fig. 9, it seems more correct to say that $Q' \propto (A - B)$ rather than $Q' \propto D$ or V_{zz} . However, we cannot utilize the results of Fig. 9 in any absolute calculations of Q because the proper equation relating all the pertinent parameters is unknown.

In view of the data obtained so far, the best value of Q for ^{53}Cr can be obtained by averaging the values found for $G(1)$, $G(2)$, and CsGa alum, giving $Q = -0.028 \pm 0.005$ b. This value is slightly lower than the value $Q = -0.035 \pm 0.005$ b predicted from the limited data presented by the gallium alums, but it is very close to the value of $|Q| = 0.026$ b predicted in the theoretical analysis of transition-metal sesquioxides by Artman.²⁰

The effective g value, g'_n , was found to be isotropic and the same for both complexes. The true nuclear g value g_n is related to g'_n as $g_n = g'_n / (1 + \sigma)$ where σ is the shielding parameter. The value of σ can be calculated from the formula²¹

$$\sigma = -5.84 \langle 1/r^3 \rangle (\Delta g / \lambda), \quad (6)$$

where Δg is the electronic- g -value shift from 2.0023, λ is the spin-orbit coupling parameter of Cr^{3+} in units of cm^{-1} , and $\langle 1/r^3 \rangle$ is the average value of $1/r^3$ for the Cr^{3+} $3d$ wave function. Using the Cr^{3+} free-ion value of $\lambda = 91 \text{ cm}^{-1}$, $\langle 1/r^3 \rangle = 3.959$ a. u., and $\Delta g = -0.024$, one finds $\sigma = 0.00638$ which gives a g_n value of -0.3145 . Since the nuclear magnetic moment is $\mu_n = g_n I$, we also find $\mu_n = -0.4718 \mu_N$ for ^{53}Cr . This is close to the handbook value²² of $-0.4735 \mu_N$ obtained from NMR studies of ^{53}Cr in solution.

The phenomenon of ferroelectricity in GAlSH did not manifest itself in a dramatic manner in the ENDOR studies. It is noted above that the spontaneous polarization in the crystal increases with decreasing temperature, and the same is true for the spin-Hamiltonian- D parameter. The ENDOR work shows that the sign of the D parameter can be related to a compression of the octahedron of waters surrounding the chromium ion, and an increase in the magnitude of D with decreasing temperature could be due to an increase in the compression. However, in the ferroelectric GAlSH crystal the Cr or Al ions are also displaced from the center of the octahedron and this effect can give a contribution to the D parameter. In this respect it is noted from the x-ray results⁷ of GAlSH at room temperature that the site which gives rise to the chromium complex $G(2)$, which has the smaller D value, actually has a slightly larger compression than the $G(1)$ site.

In conclusion, it is seen that the precise measurement of the $^{53}\text{Cr}^{3+}$ hyperfine parameters produces information which allows a more complete analysis of crystal behavior and applicability of existing theories to be made. It is evident that more work on other hydrated salts is desirable in order to check the general validity of Fig. 9 and of the hypotheses made in this study.

ACKNOWLEDGMENTS

The authors would like to thank the National Research Council, Ottawa, Canada, for financial assistance. One of us (A. L.) would also like to thank the Canadian National Research Council for a student fellowship received during the course of the work.

¹A. G. Danilov and A. Manoogian, Phys. Rev. B 6, 4097 (1972).

²A. G. Danilov and A. Manoogian, Phys. Rev. B 6, 4103 (1972).

³A. N. Holden, B. T. Matthais, M. J. Merz, and J. P. Remeika, Phys. Rev. 98, 546 (1955).

⁴E. A. Wood, Acta. Crystallogr. 9 618 (1956).

⁵A. N. Holden, M. J. Merz, J. P. Remeika, and B. T. Matthais, Phys. Rev. 101, 962 (1956).

⁶S. Geller and D. P. Booth, Z. Kristallogr. 111, 117

(1959).

⁷J. B. Schein, E. C. Lingafelter, and J. M. Stewart, J. Chem. Phys. 47, 5183 (1967).

⁸J. B. Schein, and E. C. Lingafelter, J. Chem. Phys. 47, 5190 (1967).

⁹G. S. Bogle, J. R. Gabriel, and G. A. Bottomley, Trans. Faraday Soc. 53, 1058 (1957).

¹⁰J. M. Daniels and H. Wesemeyer, Can. J. Phys. 36, 144 (1958).

¹¹G. Burns, Phys. Rev. 123, 1634 (1961).

- ¹²B. Milsch and W. Brunner, Proc. Colloque, AMPERE, 748 (1970).
- ¹³R. W. Schwartz and R. L. Carlin, J. Am. Chem. Soc. 92, 6763 (1970).
- ¹⁴H. Weaver, Varian Associates Seventh Annual NMR-EPR Workshop Notes, 1963 (unpublished).
- ¹⁵N. Laurance and J. Lambe, Phys. Rev. 132, 1029 (1963).
- ¹⁶B. R. McGarvey, J. Chem. Phys. 40, 809 (1964).
- ¹⁷B. R. McGarvey, J. Chem. Phys. 41, 3743 (1964).
- ¹⁸D. E. O'Reilly and T. Tsang, Phys. Rev. 157, 417 (1967).
- ¹⁹R. M. Sternheimer (private communication).
- ²⁰J. O. Artman, Phys. Rev. 143, 541 (1966).
- ²¹S. Geschwind, *Hyperfine Interactions*, edited by A. J. Freeman and R. B. Frankel (Academic, New York, 1967), p. 243.
- ²²*Handbook of Chemistry and Physics* (Chemical Rubber Co., Cleveland, Ohio, 1965).